

Dynamics of quantum tunneling: Effects on the rate and transition path of OH on Cu(110)Erlend R. M. Davidson,¹ Ali Alavi,² and Angelos Michaelides¹¹*London Centre for Nanotechnology and Department of Chemistry, University College London, London WC1E 6BT, United Kingdom*²*Department of Chemistry, University of Cambridge, Lensfield Road, Cambridge CB2 1EW, United Kingdom*

(Received 27 November 2009; revised manuscript received 26 February 2010; published 23 April 2010)

Recent low-temperature scanning-tunneling microscopy experiments [T. Kumagai *et al.*, Phys. Rev. B **79**, 035423 (2009)] observed the possible quantum tunneling of hydroxyl groups between two equivalent adsorption configurations on Cu(110). Here we analyze the quantum nuclear tunneling dynamics of hydroxyl on Cu(110) using density-functional theory based techniques. We calculate classical, semiclassical, and quantum-mechanical transition rates for the flipping of OH between two degenerate energy minima. The classical transition rate is essentially zero at the temperatures used in experiment and the tunneling rate along the minimum-energy path is also much too low compared to experimental observations. When tunneling is taken into account along a direct path connecting the initial and final states with only a minimum amount of the oxygen movement the transition rate obtained is in much better agreement with experiment, suggesting quantum tunneling effects cause a deviation of the reaction coordinate from the classical transition path.

DOI: [10.1103/PhysRevB.81.153410](https://doi.org/10.1103/PhysRevB.81.153410)

PACS number(s): 82.20.Xr, 68.43.Bc, 68.35.Ja

The quantum tunneling of hydrogen plays a role in a wide variety of scientific disciplines, such as the functioning of enzymes in biological processes,^{1,2} diffusion through metals,³ and high-pressure ice,⁴ to name but a few. Through well-defined experiments at surfaces it is now possible to shed light on quantum nuclear effects at the level of individual adsorbates. In particular, with low-temperature scanning-tunneling microscopy (STM) it has been possible to measure tunneling rates for a number of diffusion processes involving individual atoms and molecules. Notable examples are the measurement of the diffusion rate of H and D on a Cu surface⁵ and the diffusion of water clusters, suggested to be assisted by hydrogen bond tunneling, on a Pd surface.^{6,7} In an intriguing recent development Kumagai *et al.*⁸ interpreted STM images of hydroxyl molecules on Cu(110) as direct evidence of quantum tunneling of the hydrogen atom between two equivalent states. Individual adsorbed hydroxyl molecules were imaged as symmetric double protrusions which were suggested to correspond to a superposition of two equivalent tilted configurations either side of a symmetric transition state (TS). Since the experiments were performed at only 6 K and the barrier for the flipping process was calculated with density-functional theory (DFT) to be >0.1 eV, it was concluded that the flipping between two degenerate energy minima must be the result of rapid quantum tunneling. Estimates of the rate from Wentzel-Kramers-Brillouin (WKB) theory with the assumption that oxygen does not move during the transition and the observation of a kinetic isotope effect when deuterized OH (OD) was used, provided further evidence that the low-temperature transition is mediated by quantum tunneling. These observations are interesting and suggest that OH on Cu(110) could be a well defined and relatively simple model system for the study of quantum nuclear effects. While the DFT and WKB modeling of Kumagai *et al.* was an important step in describing this system, there are still questions that remain unanswered. The most pressing of these is the role of oxygen in the tunneling event, and the question of how the classical and quantum reaction paths may differ. In addition it is unclear how well WKB describes this particular tunneling transition. Answering these questions will not only pro-

vide deeper understanding of the quantum tunneling dynamics of adsorbed hydroxyl but will be instrumental toward developing a general understanding of the quantum effects of small molecules on surfaces.

In this work we present a brief account of our DFT based studies of the flipping of OH between two equivalent states on Cu(110). First we use the nudged elastic band (NEB) (Ref. 9) method to determine the activation energy and minimum-energy path (MEP) for the transition. We find that the barrier for the flipping process is 166 meV [145 meV including zero-point energy (ZPE) effects] and that while the H flips there is a surprisingly large movement of the oxygen. Applying classical transition-state theory to this barrier yields rates very much smaller than the experimentally measured rate and due to the combined oxygen and hydrogen movement, semiclassical estimates of the tunneling rate along the MEP are also very low. Since semiclassical methods rely on a transition path being specified, we applied a wave-function approach over the independent hydrogen and oxygen reaction coordinates to further understand the process. Overall we find that quantum tunneling can be responsible for the transition at low temperatures as long as the oxygen motion during the transition is suppressed via corner cutting of the MEP.

The DFT calculations used the CASTEP (Ref. 10) and VASP (Refs. 11–14) codes. Vanderbilt ultrasoft pseudopotentials¹⁵ were used in CASTEP and projector-augmented wave potentials¹⁶ in VASP. Wave functions were expanded in terms of a plane-wave basis set with a cutoff energy of 350 eV (CASTEP) and 415 eV (VASP). The Perdew-Burke-Ernzerhof (PBE) (Ref. 17) exchange-correlation functional was used throughout. The surface was represented as a $p(3 \times 3)$ periodic supercell, with the bottom two of the four layers fixed and 14 Å of vacuum in the z direction, normal to the surface plane. Sampling of reciprocal space was done using a $4 \times 4 \times 1$ Monkhorst-Pack \mathbf{k} -point mesh.¹⁸ These choices of cutoff energy, slab thickness, and \mathbf{k} points were made after an extensive set of convergence tests which focused specifically on accurately describing the energy barrier for the OH flipping process. These established, for example, that the barrier obtained with an eight layer setup and $8 \times 8 \times 1$ \mathbf{k} points was

TABLE I. Some relevant DFT-PBE calculated properties for OH/Cu(110). ΔE is the classical activation barrier for the OH flip. θ is the angle of the OH to the surface normal. The $\Delta_{\text{O-Cu}}$ lateral distance is the lateral displacement of the oxygen from the precise short bridge site. The values below are calculated using VASP. The values in brackets are from CASTEP.

	IS	TS
ΔE (meV)		166 (155)
O-H bond (\AA)	0.98 (0.98)	0.97 (0.97)
O-Cu bond (\AA)	1.96 (1.96)	1.95 (1.92)
θ ($^\circ$)	59.9 (62.8)	0.0 (0.0)
$\Delta_{\text{O-Cu}}$ (\AA)	0.02 (0.04)	0.00 (0.00)

only 25 meV away from that obtained with the chosen computational setup. Likewise the barrier and adsorption structures obtained with the two DFT codes were very similar (Table I). CASTEP (Ref. 10) was used to calculate the potential-energy surface (PES) for the transition, as VASP does not have nonlinear constraints.

Initially a single OH monomer was adsorbed on the Cu(110) surface. The molecule adsorbs with the oxygen near a short bridge site and the O-H tilted by about 60° to the surface normal (Table I, Fig. 1). This adsorption geometry agrees with the theoretical geometries from Kumagai *et al.*⁸ By symmetry there are two equivalent adsorption structures, as shown in Fig. 1. NEB calculations revealed that these two equivalent adsorption sites are separated by a classical barrier (ΔE) of 166 meV and the TS for this process involves a perfectly upright OH (shown in Fig. 2, image 8).

Applying classical transition-state theory, the rate for the flipping process as a function of temperature (T) is

$$\text{Rate}(T) = A e^{-\beta \Delta E}, \quad \text{where } A = \frac{\prod_{i=1}^N \nu_i^{\text{IS}}}{\prod_{i=1}^{N-1} \nu_i^{\text{TS}}}. \quad (1)$$

A is the ‘‘prefactor,’’ $\beta = (k_B T)^{-1}$, and the ν^{IS} and ν^{TS} are the initial and transition-state vibrational frequencies of the OH molecule on Cu(110). With the substrate fixed there are six modes at the initial state (IS) and five at the TS, as the lowest frequency becomes imaginary and is consequently ignored. At the 6 K used in the experiments of Kumagai *et al.*⁸ classical transition-state theory predicts a negligible rate (less

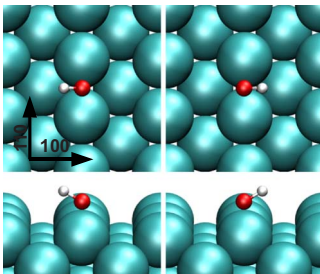


FIG. 1. (Color online) The adsorption geometry of OH on Cu(110) shown from above (top) and from the side (bottom). Two equivalent structures are possible due to symmetry. In our discussion we will refer to the image on the left as the IS and the image on the right as the FS.

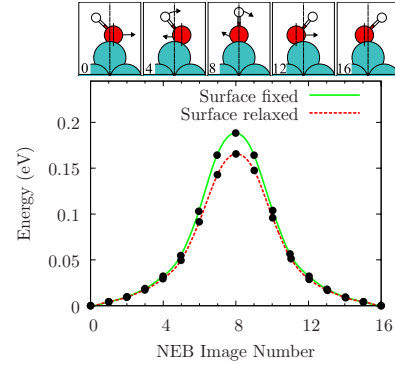


FIG. 2. (Color online) MEP obtained from a 15-image NEB calculation for the hydroxyl flip process on Cu(110). The red (dashed) and green (solid) curves correspond to the converged MEP with the top two layers of the surface relaxed or fixed in their bulk truncated configuration, respectively. The relaxed and fixed models predict transition barriers of 166 and 187 meV, respectively. The cartoons at the top of the graph are schematic illustrations of how the molecule moves during the flipping process, with the arrows indicating how the molecule moves from one step to the next. Although the difference in position between the O atom in the initial and final states is very small along the MEP the oxygen undergoes a large displacement before passing through the transition state. It is this supplementary oxygen movement which greatly suppresses the tunneling rate along the MEP.

than 10^{-100} s^{-1} for OH and OD). Therefore, as Kumagai *et al.* discussed, the double depressions achieved in one low-temperature STM image suggest that the molecule tunnels between two equivalent structures. Employing a simple harmonic semiclassical approximation to the transition state suggests quantum effects should be relevant below about 80 K for OD or 100 K for OH.¹⁹ This is much higher than the 6 K used in the experiments and so quantum tunneling effects need to be considered.

One of the simplest methods to approach tunneling is the WKB approximation. This gives an estimate for the rate,

$$\text{Rate} = \nu e^{-2/\hbar \int_0^a dx \sqrt{2m[V(x) - E]}}, \quad (2)$$

where ν (in per second) is the initial-state frequency along the reaction coordinate, a is the transition path length {chosen such that $[0, a]$ corresponds with nonclassical region where $E < V(x)$ }, m is the mass of the tunneling species, and \hbar is Planck’s constant over 2π . $V(x)$ and E are the potential barrier and initial energy, respectively. Here E is the ZPE contribution.²⁰ Within WKB a transition path must be *a priori* defined, however since for the process considered here several different, yet still feasible, paths exist this is an immediate drawback. Nonetheless it is obvious to start by choosing the MEP. If we solve Eq. (2) for tunneling of OD or OH along the MEP (Ref. 21) we obtain a rate of less than 10^{-6} s^{-1} . This is a much lower rate than the one determined in experiment.

Previous work has shown that a deviation from the MEP is sometimes preferred in transitions involving several different masses²² and so to better understand the transition and possible alternative tunneling paths, we mapped out the PES for hydrogen and oxygen motion during the transition. This

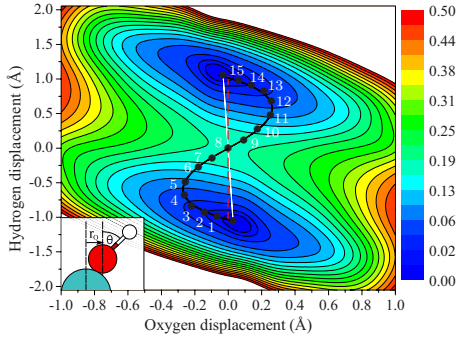


FIG. 3. (Color online) Potential energy surface in electron volt for the hydroxyl flip process on the bulk truncated Cu(110) surface as a function of oxygen and hydrogen displacement. This was generated by constraining the angle of the OH to surface normal (θ in the inset) and fixing the oxygen position at each displacement in the Cartesian x and y axes, both parallel to the surface. At each displacement ($r_O = \Delta_{O-Cu}$) the hydroxyl was free to relax both by moving in the z direction (normal to the surface plane) and by varying the OH bond length. A total of 90 DFT calculations were performed and the results interpolated by means of a cubic spline to a finer mesh. The MEP is shown as a black curve and each image (except for the initial and final states) is numbered. Bead number eight is the transition state. The white solid line is the direct path joining the initial and final configurations with minimal movement of the oxygen. The dashed red line with no oxygen movement represents the WKB tunneling path used by Kumagai *et al.*

was done on the fixed Cu(110) surface since it reduces the transition to just two degrees of freedom (lateral oxygen movement and displacement of the hydrogen) and the barrier is only changed by ~ 20 meV. The calculated PES is shown in Fig. 3. If we use the classical transition path (Fig. 2, black line in 3) with the total mass of the OH molecule and the center of mass as the reaction coordinate, the transition rate is approximately 10^{-8} s $^{-1}$ for OD (10^{-6} s $^{-1}$ for OH) similar to that obtained on the relaxed surface and still a far lower rate than experimental observations suggest. Assuming the hydrogen moves in a circular path and that the oxygen is completely stationary (as done originally by Kumagai *et al.*), the WKB rate is approximately 10^4 s $^{-1}$ for OD (10^6 s $^{-1}$ for OH). Therefore movement of the oxygen during the transition has a substantial quenching effect on the rate. Another possibility is that the oxygen neither remains completely stationary nor follows the MEP but instead takes a “direct” path from its IS to its final state (FS) position (the straight solid white line in Fig. 3). This results in a simple reaction coordinate which is orthogonal to the MEP with a total oxygen displacement of just 0.04 Å, compared to about 1 Å along the MEP. Using this path with WKB we evaluate a tunneling rate of about 10^5 s $^{-1}$.

So far we see that tunneling is certainly possible at the temperature used in experiments. The calculation of the rates from WKB is complicated because it requires the prior selection of the reaction path and as we have just seen this choice can have a huge impact on the obtained rate. Explicit calculation of the wave functions from the PES allows for an estimate of the transition rate without choosing a particular reaction coordinate.

We can write the time-independent Schrödinger equation in terms of the hydrogen and oxygen movement,

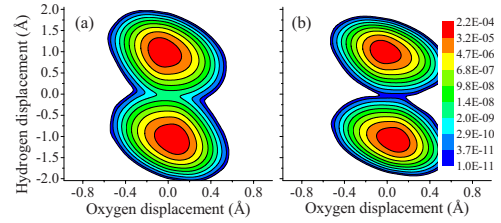


FIG. 4. (Color online) Probability densities of (a) OH and (b) OD position on Cu(110) at 6 K. Both graphs show a double-peaked structure, with a small probability at the transition state (the transition state is where oxygen and hydrogen displacements are both zero). A logarithmic scale is used to emphasize the probability at the barrier region.

$$\left[-\frac{\hbar^2}{2m_H} \frac{\partial^2}{\partial r_H^2} - \frac{\hbar^2}{2m_O} \frac{\partial^2}{\partial r_O^2} + V(r_H, r_O) \right] \psi(r_H, r_O) = E\psi(r_H, r_O), \quad (3)$$

where r_H and r_O are the hydrogen and oxygen degrees of freedom, and m_H and m_O are the masses of hydrogen (or deuterium) and oxygen, respectively. $V(r_H, r_O)$ is the potential-energy surface (Fig. 3).²³ The nuclear wave function $\psi(r_H, r_O)$ was expanded in a plane-wave basis, up to a cutoff of 5 Ry. The Hamiltonian is solved using an iterative Lanczos algorithm,^{24,25} in which the kinetic-energy operator is applied in Fourier space, and the potential-energy operator is applied in real space. The result is a sequence of energy levels and their corresponding wave functions (eigenvalues and eigenvectors of the discretized Hamiltonian). At a particular temperature the probability density (P) will be a superposition of all the calculated eigenstates weighted by the Boltzmann factor,

$$P = \sum_{i=1} |\psi_i|^2 \frac{e^{-\beta E_i}}{Z}, \quad Z = \sum_{i=1} e^{-\beta E_i}, \quad (4)$$

where the index i runs over consecutive eigenstates, the $\{\psi_i\}$ and $\{E_i\}$ are eigenvectors and eigenvalues from the Lanczos procedure, respectively. The results from the wavelike calculations of the density functions for OH and OD are shown in Fig. 4. The probability densities exhibit a double-peaked structure with the two peaks centered on the two minima of the PES (Figs. 3 and 4). By appealing to a semiclassical transition-state theory approximation, we can relate the probability of a tunneling event to the ratio of probability densities at the initial (r_{IS}) and transition (r_{TS}) states,

$$\text{Rate} = \nu \frac{P(T, r_{TS})}{P(T, r_{IS})}. \quad (5)$$

The initial-state frequency (ν) is essentially the number of transition attempts. Equation (5) has the usual limitations of conventional transition-state theory, in particular, recrossing of the saddle point is not considered and we are assuming the initial harmonic frequency along the path directly connecting and IS and TS is valid. Using the calculated frequency along the PES reaction coordinate of $\nu = 2.98 \times 10^{12}$ s $^{-1}$ for OD in the initial state ($\nu = 3.17 \times 10^{12}$ s $^{-1}$ for OH) we calculate rates of $\sim 1 \times 10^5$ s $^{-1}$ for OD and $\sim 1 \times 10^8$ s $^{-1}$ for OH

TABLE II. Rates (in per second) for the OH and OD flipping process on Cu(110) at 6 K. The classical transition state theory (TST) rate is the one obtained from the Arrhenius equation [Eq. (1)] using the classical energy barrier. The “WKB MEP” rate is calculated along the classical transition path. The “O-stationary” transition is represented by the dashed red line in Fig. 3. The “WKB direct” transition is the one shown by the solid white line in Fig. 3. The transition rate labeled “wave function” is the one obtained from Eq. (5). Rates include a contribution from ZPE.

	OH	OD
Experiment		$0.9 \times 10^3 \pm 0.4 \times 10^3$
Classical TST	$< 10^{-100}$	$< 10^{-100}$
WKB MEP	7×10^{-8}	$< 10^{-10}$
WKB O stationary	3×10^6	1×10^4
WKB direct	7×10^5	1.9×10^3
Wave function	1×10^8	1×10^5

(Table II). Thus the wave-function calculations also clearly indicate that rapid flipping is possible. The rate predicted by this method is greater than that to come from experiment and WKB (when there is minimal or no displacement of oxygen). This overestimation may be a drawback of the reduced dimensionality of the wave-function model.

The WKB calculations predicted a corner-cutting deviation from the MEP and further evidence for this can be seen with wave-function calculations with a fictitious mass. Varying the oxygen mass has relatively little effect on the transition probability compared with the change from OD to OH, suggesting that oxygen plays a small role in the transition. For example, if the mass of oxygen is increased to 32 a.u. the transition probability is only reduced to 10^{-6} (compared with 10^{-5} for OH).

Having used DFT, WKB and wave-function modeling to examine the flipping of OH between two equivalent adsorption geometries, we can now further understand the STM result of Kumagai *et al.* Quantum tunneling can make the flipping process possible at the low temperatures used, how-

ever for tunneling to occur at an appreciable rate there must be a change in the reaction pathway of the classical transition. In particular, the superfluous zigzag movement of oxygen during the transition must be minimized. One way this can happen is for the oxygen to remain completely stationary. Another more likely scenario is a direct transition (solid white line in Fig. 3) since the path length is significantly shortened and the barrier height is identical to the classical transition. The fact that the path length can be considerably shortened but the transition still proceeds through the lowest energy transition state is a particularly unusual and noteworthy feature of this system. In general the dynamics of a classical transition for hydrogenated molecules such as OD (OH) will show considerable movement of the heavy species, due to the MEP following the lowest frequency mode. For these systems it may be expected that tunneling yields a much higher transition rate along a path orthogonal to the MEP, which reduces movement of the heavy species and should couple the new reaction coordinate to a harder vibrational mode. This is similar to the large curvature tunneling path methods discussed for heavy-light-heavy nuclei.²²

We have used various techniques to compute rates for the hydroxyl flipping process on Cu(110). All of these methods have drawbacks but they do indicate that tunneling is possible under a change in the reaction coordinate from the MEP. Ideally a complete treatment of this system would include the full dimensionality and anharmonic effects, such as is possible using path-integral molecular dynamics.

A.M.’s work is supported by the European Research Council, the EURYI scheme, and the EPSRC. We are grateful to the London Centre for Nanotechnology and UCL Research Computing for computational resources. This work also made use of the facilities of HECToR, the U.K.’s national high-performance computing service, which is provided by UoE HPCx Ltd. at the University of Edinburgh, Cray Inc. and NAG Ltd., and funded by the Office of Science and Technology through EPSRC’s High End Computing Programme. We also thank J. Carrasco for providing some initial structures.

¹A. Kohen *et al.*, *Acc. Chem. Res.* **31**, 397 (1998).

²A. Kohen *et al.*, *Nature (London)* **399**, 496 (1999).

³Y. Fukai, *The Metal-Hydrogen System: Basic Bulk Properties* (Springer-Verlag, Berlin, 2005).

⁴M. Benoit *et al.*, *Nature (London)* **392**, 258 (1998).

⁵L. J. Lauhon *et al.*, *Phys. Rev. Lett.* **85**, 4566 (2000).

⁶V. A. Ranea *et al.*, *Phys. Rev. Lett.* **92**, 136104 (2004).

⁷T. Kumagai *et al.*, *Phys. Rev. Lett.* **100**, 166101 (2008).

⁸T. Kumagai *et al.*, *Phys. Rev. B* **79**, 035423 (2009).

⁹G. H. J. Mills *et al.*, *Surf. Sci.* **324**, 305 (1995).

¹⁰S. J. Clark *et al.*, *Z. Kristallogr.* **220**, 567 (2005).

¹¹G. Kresse *et al.*, *Phys. Rev. B* **47**, 558 (1993).

¹²G. Kresse *et al.*, *Phys. Rev. B* **49**, 14251 (1994).

¹³G. Kresse *et al.*, *Comput. Mater. Sci.* **6**, 15 (1996).

¹⁴G. Kresse *et al.*, *Phys. Rev. B* **54**, 11169 (1996).

¹⁵D. Vanderbilt, *Phys. Rev. B* **41**, 7892 (1990).

¹⁶P. E. Blöchl, *Phys. Rev. B* **50**, 17953 (1994).

¹⁷J. P. Perdew *et al.*, *Phys. Rev. Lett.* **77**, 3865 (1996).

¹⁸H. J. Monkhorst *et al.*, *Phys. Rev. B* **13**, 5188 (1976).

¹⁹Using the Landau-Lifshitz equation, $T_c = \hbar \nu^{TS} / (2\pi k_B)$, where ν is the (imaginary) frequency at the transition state ($4.3 \times 10^{12} \text{ s}^{-1}$ for OH and $4.1 \times 10^{12} \text{ s}^{-1}$ for OD), k_B is Boltzmann’s constant, and $\hbar = h(2\pi)^{-1}$. This is discussed in M. J. Gillan, *J. Phys. C* **20**, 3621 (1987).

²⁰The zero-point energy contribution to the activation energy barrier is determined from the initial-state and transition-state frequencies. The ZPE of a state is $E^{ZPE} = \frac{\hbar}{2} \sum_i^N \nu_i$, where N is the number of vibrational modes (six at the initial state and five at the transition state). The effect of ZPE on the barrier is given by $E_{TS}^{ZPE} - E_{IS}^{ZPE}$.

²¹Using the full OH (or OD) mass along a reaction coordinate given by the movement of the center of mass of the molecule.

²²B. C. Garrett *et al.*, *J. Chem. Phys.* **78**, 4400 (1983).

²³ r_H is determined as the arc length of the hydrogen from the surface-normal position using $r_H = r\pi\theta/180$, where r is the OH bond length.

²⁴M. Dyer *et al.*, *ChemPhysChem* **6**, 1711 (2005).

²⁵G. Groenenboom *et al.*, *J. Chem. Phys.* **92**, 4374 (1990).